Synthesis of WO_3@graphene composite for fructose degradation

Zhenya Jiang, Yao Wang, Lifeng Yan*

Department of Chemical Physics, iCHEM, University of Science and Technology of China, Jinzai Raod 96, Hefei, 230026, Anhui, China

*Corresponding author: Tel: (+86) 551-63606853; E-mail: lfyan@ustc.edu.cn

Received: 04 February 2017, Revised: 01 April 2017 and Accepted: 04 April 2017

DOI: 10.5185/amlett.2017.1660
www.vbripress.com/aml

Abstract

WO_3@Graphene (WO_3@GR) nanocomposite has been synthesized by using a simple sonochemical method, and the phosphotungstic acid was used as the source of the WO_3 nanoparticles. The new catalyst was analyzed by means of FT-IR, XRD, TEM, and SEM-EDX. FT-IR spectrum of the new material reveals that sulfonic acid groups existed on the surface of graphene nanosheets. In addition, TEM image of WO_3@GR indicates that the WO_3 nano-particles in size of 5-10 nm have an uniform distribution on the surface of the graphene nanosheets. The as-prepared nanocomposite can be used as a catalyst for biomass conversion, and the catalytic hydrolysis of fructose was carried out at different experiment conditions, such as reaction temperature, reaction time and catalyst dosage. HPLC has been used to measure the compounds in product and their yield. It was found that the major products include HMF, formic acid, lactic acid, acetic acid, and maleic acid, and the maximum yield is 43.25% when the reaction was carried out at 160 ^oC with the ratio of fructose to catalyst is 8 in the presence of 20 ml of water for 2h. The results reveal that the WO_3@GR nanocomposite is a potential catalyst for biomass conversion.

Keywords: Graphene, WO_3, nanocomposite, catalyst, sugar, degradation.

Introduction

Biomass is regarded as the alternative feedstock for non-renewable fossil resource decreasing sharply in the past several decades,[**1**] especially for sustainable production of fuels and chemicals [**2**]. Monosccharide, such as glucose and fructose are as the most abundant monosaccharides of promising biomass resource, which can be obtained from cellulose by different reaction system such as enzymes, dilute acids, and supercritical water and isomerization. In addition, degradation of them has attracted much attention because they can be converted efficiently into various highly valuable platform chemicals such as 5-hydroxymethylfurfural (HMF), lactic acid, and formic acid [**3**]. HMF is a furan derivative contains hydroxylmethyl group and aldehyde groups, which can be used for synthesis of a variety of plastics, and other fine chemicals [**4-7**]. The key point of the conversion to value-added platform chemicals is catalysts, which has been investigated by many researchers [**8**].

Carbon supported metal catalysts are well known in both industrial and laboratory. As a number of carbon family, graphene has been widely used in many reactions for preparation of catalyst owing to its advantages such as large surface area, excellent mechanical properties and good conductivity [**9**]. Various kinds of graphene-based materials have been synthesized for different reactions such as degradation of biomass resources, photocatalysis, and electrochemical catalysis, etc [**10**]. WO_3@graphene nanocomposites have been also prepared as catalyst for photocatalysis, such as for degradation of 1-Naphthol **[11, 12**] **[13, 14**]. Interesting, WO_3 is also an efficient catalyst for biomass conversion, for example, WO_3 nanoparticles supported by Ru/C or MoO_3 catalysts showed excellent catalysis activity for degradation of cellulose, glucose or glycerol [**15-17**].

Here, WO_3@graphene nanocomposite has been synthesized and was used for catalytic conversion of fructose to valuable platform chemicals.

Experimental

Materials

Graphite powder, phosphotungstic acid, sodium nitrate ($NaNO_3$), sulfuric acid (98% H_2SO_4), hydrogen peroxide (30% H_2O_2), hydrochloric acid (12M HCl), ethanol, fructose ($C_6H_{12}O_6 \cdot H_2O$) were purchased from Sinopharm Chemical Reagent Co.Ltd., and were used directly without further purification. Ultrapure water (18 MΩ) was produced by a Millipore System (Millipore Q, U.S.A.).

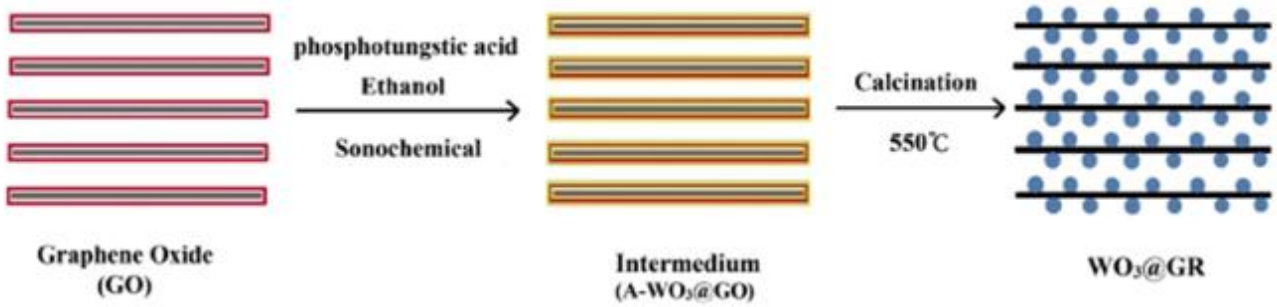

Fig.1. Synthesis of the WO_3@GR nanocomposite.

Material synthesis / reactions

Graphite oxide (GO) was prepared from natural graphite by the well-known modified Hummers method [**11**]. WO_3@graphene (WO_3@GR) was synthesized by using ultrasound method as shown in **Fig. 1**. In brief, 0.25g GO powder was added into 20 ml of ultrapure water under stirring, and then 0.2-1.2g of phosphotungstic acid and 10 ml ethanol was added into the solution slowly, and the mixture was carried out reaction under strong ultrasound (500-600 W) for 3h. After reaction, the as-prepared product was centrifuged and washed by ethanol several times. Finally, WO_3@GR powder was obtained by freezing drying.

The reaction of degradation of fructose was carried out in a high-pressure vessel (50ml, Parr Instrument Company, USA), and it is equipped with a magnetic stirrer and a program temperature controller. After reaction, the reaction solution was filtered and a yellow solution was obtained, then the solution was diluted with ultrapure water to 100ml. Next, the as-prepared product was filtered by the syringe membrane filter, which included small molecule organic acids and HMF, and then it can be directly analyzed by using HPLC equipped with an UV/VIS detector (SPD-20A, Japan).

Characterizations

Fourier transform infrared (FT-IR) spectra of the samples were analyzed by a FT-IR spectrometer (Tensor 27, Bruker, Germany). Thermogravimetric Analyzer (Q5000IR, TA, USA) was used to measure the thermal stability of as-prepared samples, and all of the measurements were carried out under nitrogen gas over a temperature range of 25-800 ^oC with a ramp rate of 10 ^oC min^{-1}. The surface topography of samples was recorded by a Scanning Electron Microscope (SEM, Sirion200, FEI, Netherlands). TEM images of samples were taken by a High Resolution Transmission Electron Microscope (TEM, JEOL-2010, Japan).

Results and discussion

Fig. 2 shows the FT-IR spectra of GO and the as-prepared nanocomposite. For rGO, the characteristic peaks appear for C=O (1735 cm^{-1}), aromatic C=C (1622 cm^{-1}), carboxy C-O (1414 cm^{-1}), epoxy C-O (1228 cm^{-1}), and C-O (1116 cm^{-1}), indicating an efficient reduction of GO during the reaction. For the composite, several new peaks appeared at 986.07 cm^{-1}, 889.96 cm^{-1}, and 811.65 cm^{-1}, which are the characteristic signal of symmetric stretching vibration modes of W-O-W bonds, and the original peaks at 1042 cm^{-1} shifts to 1080.29 cm^{-1}, corresponds to the stretching vibration modes of C-O-W bond. The FT-IR results reveal the formation of a composite of WO_3 and reduced graphene oxide.

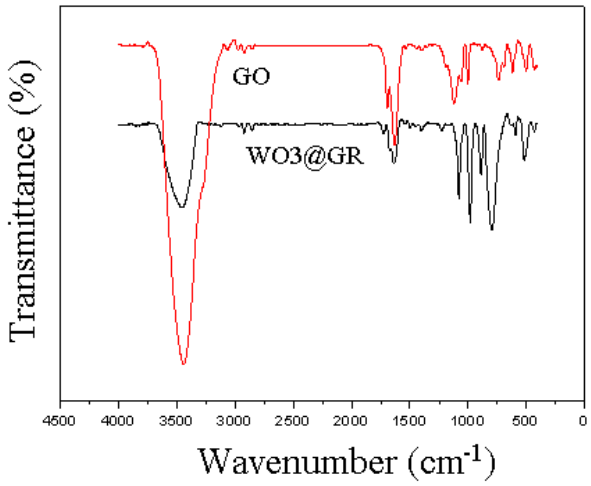

Fig. 2. FT-IR spectra of GO and WO_3@GR.

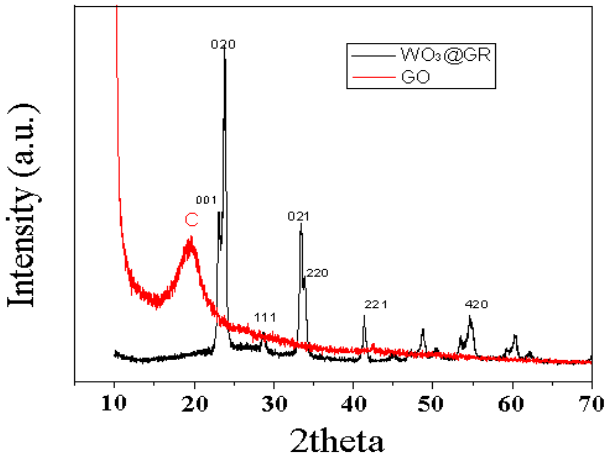

Fig. 3. XRD patterns of GO and WO_3@GO.

The crystal phase structure of the as-prepared composite was characterized by X-ray diffractometer. **Fig. 3** shows the typical XRD patterns of GO and the composite prepared by loading 20 wt% of WO_3, respectively. For, GO powder, there appears a wide peak

at around 10.4°, revealing that the interlayer spacing of GO nanosheets was about 0.8nm. However, after growth of WO_3 nanoparticles on the surface of the GO nanosheets, the broad peak disappeared, indicating the expanded of the stacking of GO nanosheets during reaction. In the curve, a series of diffraction peaks appeared which can be indexed as WO_3 nanocrystalline. The size of the WO_3 nanoparticles calculated by means of XRD patterns are about 5.8nm, indicating the success synthesis of the nanocomposite.

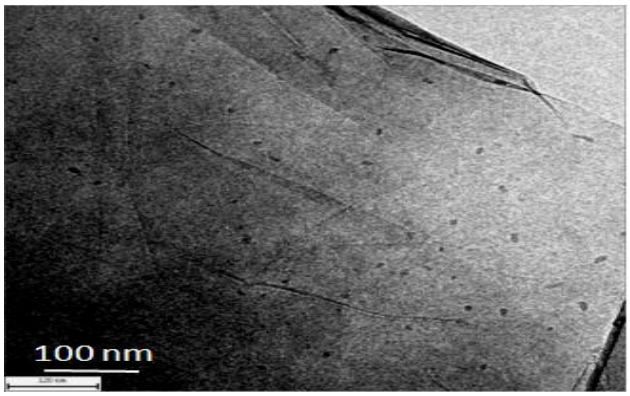

Fig. 4. TEM image of the as-prepared WO_3@GR nanocomposite.

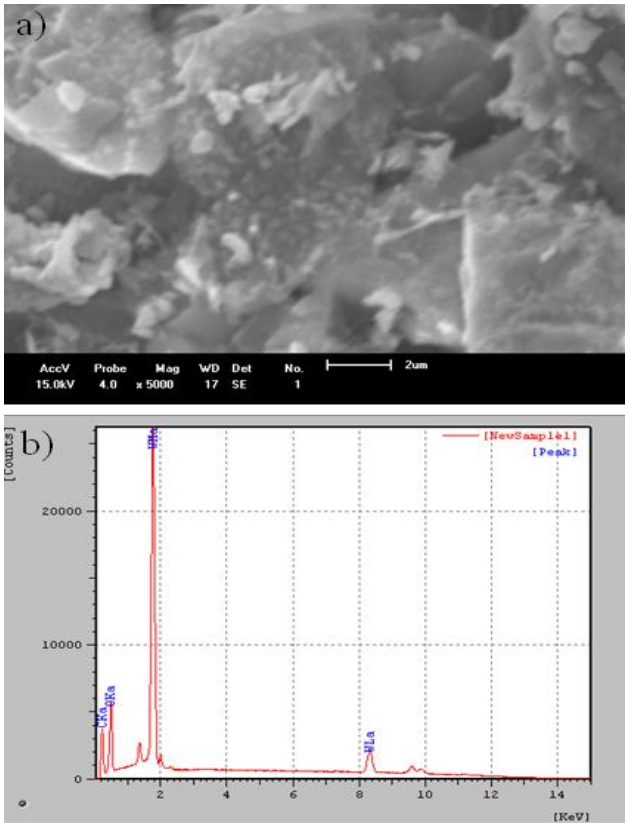

Fig. 5. (a)SEM image and (b) EDX curve of the as-prepared WO_3@GR nanocomposite.

TEM was used to directly measure the size of the WO_3 nanoparticles on the surface of reduced graphene oxide, as shown in **Fig. 4**, there forms plenty of WO_3 nanoparticles on reduced GO nanosheets when the loading of WO_3 is about 5%, and the size of the nanoparticles is about 5-10nm, which is consistent with the result of XRD measurement, also indicating the formation of the nanocomposite of WO_3@GR.

The structure of the as-formed product with high WO_3 loading (20 wt%) was also measured by means of SEM-EDX, as shown in **Fig. 5**. Clearly, some nanoparticles can be found on the surface of reduced GO nanosheets with an homogeneous dispersion, and the EDX analysis showed that the main chemical elements of the sample are C and W. The results reveal that WO_3 in the complex is in the form of nanoparticles which anchored homogeneously onto the surface of reduced GO nanosheets.

Table 1. Effect of reaction temperature on yields of products.

T (°C)	FA (wt%)	LA (wt%)	AA (wt%)	MA (wt%)	HMF (wt%)	Total yield (wt%)
140	14.48	7.14	8.74	0.05	4.52	34.93
160	13.93	13.2	9.7	0.056	6.36	43.25
180	12.62	12.11	8.78	0.064	4.08	37.65
200	8.48	14.1	5.93	0.2	2.84	31.01

Table 2. Effect of reaction time on yields of products.

Time (h)	FA (wt%)	LA (wt%)	AA (wt%)	MA (wt%)	HMF (wt%)	Total yield (wt%)
1	12.29	7.84	6.75	0.076	7.00	33.96
2	13.93	13.2	9.7	0.056	6.36	43.25
3	11.93	13.14	11.46	0.096	4.06	40.69
4	11.07	12.35	10.59	0.095	3.36	37.47

Table 3. Effect of catalyst dosage on yields of products from fructose.

Cat. (mg)	FA (wt%)	LA (wt%)	AA (wt%)	MA (wt%)	HMF (wt%)	Total yield (wt%)
5.4	11.89	10.98	8.2	0.061	6.87	38.0
8.0	13.0	10.64	8.76	0.065	6.22	38.69
10.3	13.93	13.2	9.7	0.056	6.36	43.25
15.6	11.46	12.93	8.5	0.11	7.76	40.76

Fructose: 0.085g

The above studies reveal the successful preparation of WO_3@GR nanocomposite, and it has been used as catalyst for the degradation of monosaccharide such as fructose to small organic acids in aqueous phase. All these substrates can be converted completely by hydrothermal reaction in the presence of catalyst, and the results of the effect of temperature were listed in **Table 1**. Clearly, the major products of the reaction include formic acid (FA), lactic acid (LA), acetic acid (AA), maleic acid (MA), and 5-hydroxymethylfurfural (HMF). Reaction temperature is a key factor, and the optimal temperature should be 160 °C with total yield of the above compounds 43.25%, and the major compounds are formic acid and lactic acid.

Table 2 lists the results of the conversion of fructose over WO_3@GR (10%wt) catalyst for different reaction time, and the yield of lactic acid increased from 1h to 2h, and then changed little. For acetic acid, the maximum yield appeared at 3h, while for HMF the shorter reaction time should be better. The total yield reaches the maximum at 2h. The effect of catalyst dosage on the reaction was also studied and the results were list in **Table 3**.

Conclusion

Reduced GO nanosheets has been used as the support for WO_3 nanoparticle, and the as-prepared catalyst was used to degrade fructose to organic compounds, such as lactic acid, formic acid, acetic acid, etc. The yields of the main products reach up 43%. The as-prepared new catalyst has potential application in scale production of small molecular acids from biomass.

Acknowledgements

This work was supported by the National Natural Science Foundation of China (No. 51373162 and 51673180)

Author's contributions

Conceived the plan: ly Performed the expeirments: zyj and yw; Data analysis: ly and zj yz; Wrote the paper: zj and ly. Authors have no competing financial interests.

References

1. Jin, F.; Enomoto, H. *Energy Environm. Sci.* **2011**, *4*, 382. **DOI:** 10.1039/c004268d
2. Gallezot, P. Chem. Soc. Rev. **2012**, *41*, 1538. **DOI:** 10.1039/c1cs15147a
3. Deng, T. S.; Cui, X. J.; Qi, Y. Q.; Wang, Y. X.; Hou, X. L.; Zhu, Y. L. *Chem. Commun.* **2012**, *48*, 5494. **DOI:** 10.1039/c2cc00122e
4. Wang, Y. X.; Pedersen, C. M.; Deng, T. S.; Qiao, Y.; Hou, X. L. *Bioresource Technol.* **2013**, *143*, 384. **DOI:** 10.1016/j.biortech.2013.06.024
5. Zhao, H.; Holladay, J. E.; Brown, H.; Zhang, Z. C. *Science*, **2007**, *316*, 1597. **DOI:** 10.1126/science.1141199
6. Wei, Z. J., Li, Y., Thushara, D., Liu, Y.X., Ren, Q.L., . *J. Taiwan Inst. Chem. Eng.*, **2011**, *42*, 363
7. Hu, S.; Zhang, Z.; Song, J.; Zhou, Y.; Han, B. *Green Chem.* **2009**, *11*, 1746. **DOI:** 10.1039/B914601F
8. Choudhary, V.; Pinar, A. B.; Lobo, R. F.; Vlachos, D. G.; Sandler, S. I. *Chemsuschem*, **2013**, *6*, 2369. **DOI:**10.1002/cssc.201300328
9. Machado, B. F.; Serp, P. *Cat. Sci. Technol.* **2012**, *2*, 54. **DOI:** 10.1039/c1cy00361e
10. Verma, D.; Tiwari, R.; Sinha, A. K. *Rsc Adv.* **2013**, *3*, 13265. **DOI:** 10.1039/c3ra41025k
11. Azimirad, R.; Safa, S. *Mater. Chem. Phys.* **2015**, *162*, 686. **DOI:** 10.1016/j.matchemphys.2015.06.043
12. Hajishafiee, H.; Sangpour, P. *Nano*, **2015**, *10*. **DOI:** 10.1142/s1793292015500721
13. Huang, H.; Yue, Z.; Li, G.; Wang, X.; Huang, J.; Du, Y.; Yang, P. *J. Mater. Chem. A*, **2013**, *1*, 15110. **DOI:** 10.1039/c3ta13433d
14. Li, F.; Tian, X.; Yuhong, Z.; Jun, Y.; Aiwu, W.; Zhong, W. *Ceramics Int.* **2015**, *41*, 5903. **DOI:** 10.1016/j.ceramint.2015.01.022
15. Cao, Y.L.; Wang, J.W.; Kang, M.Q.; Zhu, Y.L. *J. Fuel Chem.Technol.* **2016**, *44*, 845. **DOI:** 10.1016/s1872-5813(16)30038-x
16. Changhai, D.; Zhiwen, Z. *Adv. Mater. Res.* **2013**, *365*, 724.
17. Li, G.; Pidko, E. A.; Hensen, E. J. M. *Acs Cat.* **2016**, *6*, 4162. **DOI:** 10.1021/acscatal.6b00869

